# Search for Cosmic Ray Anisotropy with the Alpha Magnetic Spectrometer on the International Space Station

G. La Vacca and the AMS-02 Collaboration

*INFN Milano-Bicocca, Piazza della Scienza 3, 20125 Milano, Italy*

The search for cosmic ray anisotropy has been performed using particles collected by the Alpha Magnetic Spectrometer after the first five years of operation. The positron to electron ratio is consistent with isotropy at all energies and angular scales. The limit on the dipole anisotropy at the 95% confidence level for energies above 16 GeV is $\delta < 0.020$ for positrons and $\delta < 0.006$ for electrons. In the case of high rigidity protons the upper limit in the rigidity range from 80 to 1800 GV is $\delta < 0.003$. No indication of seasonal excess is observed for all particle species within the present statistics.

Recent precise measurements of Cosmic Ray (CR) fluxes performed by the Alpha Magnetic Spectrometer (AMS-02) revealed many structures in the CR spectra that are fundamental for the understanding of the CR origin problem. In particular the proton spectral shape showed a hardening of the spectral index at rigidities above 100 GV [1]. Besides the slope of the positron fraction decreases logarithmically with energy above 30 GeV and above 200 GeV the positron fraction is no longer increasing with energy [2]. This behaviour originates from the electron and positron fluxes dependence on energy. Above 20 GeV and up to 200 GeV the electron flux decreases more rapidly with energy than the positron flux, that is, the electron flux is softer than the positron flux [3].

All these features cannot be fully explained within the current physical knowledge. However they may be connected to new phenomena which, in principle, could induce some degree of anisotropy in the CR arrival directions. Therefore, besides CR spectra, it is worth to characterize the properties of the observed angular distribution of the galactic CR in order to provide complementary information for constraining both the origin and the propagation mechanism of CRs in the heliosphere and in the Galaxy.

In this work we analized the sample of the first five years of the AMS-02 data, searching for relative anisotropies in the galactic CR incoming directions. The analysis has been performed both at the detector altitude and after reconstructing the CR trajectories in the geomagnetic field. A systematic study of the seasonal dependence of the anisotropy has been performed.

## I. THE AMS-02 DETECTOR

AMS-02 is a TeV multipurpose CR detector, designed to conduct a long term mission (about 14 years). It was installed at nearly 400 km altitude on board of the International Space Station (ISS) on 19 May 2011 and since then it is operating 24/7, so far collecting more than 40 billion events of galactic CR.

The detector [4] consists of nine planes of precision silicon tracker with two outer planes, 1 and 9, and the inner tracker, planes 2 to 8; a transition radiation detector (TRD); four planes of time of flight (TOF) counters; a permanent magnet; an array of anticoincidence counters (ACC), inside the magnet bore; a ring imaging Čerenkov detector (RICH); and an electromagnetic calorimeter (ECAL).

## II. DATA SELECTION

The quality criteria for the electron and positron selection for this analysis follows that described in [3] and in [2]. The reduction of the proton background in the identification of the positron and electron samples is achieved by means of the TRD, the ECAL and the tracker. Events are selected by requiring a track in the TRD and in the tracker, a cluster of hits in the ECAL, and a measured velocity $\beta \sim 1$ in the TOF consistent with a downward-going Z= 1 particle. Protons are rejected by requiring a good energy-momentum matching and explicit cuts on the ECAL and TRD estimators. The remaining sample contains 70000 primary positrons, 920000 electrons and a negligible amount of protons.

The selected events are grouped into 5 cumulative energy ranges from 16 to 350 GeV according to their measured energy in the ECAL. The minimum energies are 16, 25, 40, 65 and 100 GeV, respectively.

Proton selection follows the one described in [1]. The first step of the selection requires the preselection of events in which the velocity was measured by at least three TOF layers being consistent with downgoing particles, and the linearly extrapolated trajectory of the TOF hit positions passing both tracker layer 1 and 9. Then further cuts are made requiring the charge consistency with Z= 1 particle and requiring the track to pass through layer 1 and 9 and to satisfy additional track fitting quality criteria.

In addition, to select only primary CRs, well above the geomagnetic cutoff, the measured rigidity is required to be greater than 1.2 times the maximum geomagnetic cutoff within the AMS field of view.

## III.   METHODOLOGY AND SKY MAPS

The CR arrival directions are used to build sky maps in galactic coordinates $(l, b)$ containing the number of observed particles. The sky maps are built using the HEALPix [9] pixelization, which guarantees a regular sampling of the CR angular distribution. The maps corresponding to electrons and positrons in the energy range from 16 to 350 GeV are displayed in Fig. 1. From this figure it is clear that AMS-02 is able to perform a nearly full-sky observation and therefore a three-dimensional measurement of the tiny CR anisotropy signals. Moreover, due to the ISS orbit inclination of 51.6° relative to the Earth equator, combined with the AMS-02 attitude on the ISS, the sky coverage of the AMS-02 exposure is non-uniform, being larger in the North Geographic Pole region than in the South. All CR species share the same exposure property.

The analysis of anisotropies requires the creation of reference maps that represent the null-hypothesis or the isotropic sky as seen by the detector. In this work we present results about the study of the *relative* anisotropy in which other CR species are used as reference for the sample of interest, such as electrons or protons for positrons. Another option discussed here is the use of a CR distribution as reference for the same species but at a different rigidity bin, such as low rigidity protons as reference for high rigidity protons.

Using the distribution of events in the reference maps, a likelihood fit procedure has been set up to compare the species under study to the reference sky map. The fit also takes into account the differences in the exposure for different rigidities due to the different geomagnetic cutoff. This procedure proved to be stable against different map resolutions and sample statistics. The flux is expanded in spherical harmonics

$$\frac{\phi_i - \langle \phi_i \rangle}{\langle \phi_i \rangle} = \sum_{\ell=0}^{\ell_{max}} \sum_{m=-\ell}^{\ell} a_{\ell m} Y_{\ell m}(l_i, b_i), \qquad (1)$$

where $(l_i, b_i)$ is the position of the $i^{th}$ pixel in galactic coordinates. The dipole for $\ell = 1$ is fully described by three orthogonal functions aligned in galactic coordinates with interesting directions: $Y_{10}$ along the North-South (NS) direction perpendicular to the galactic plane, $Y_{11}$ along the Forward-Backward (FB) direction with respect to the galactic center and $Y_{1-1}$ along the East-West (EW) direction tangent to the orbit of the sun around the galactic center. It is then worth to study these three directions both separately and combined to determine the total omnidirectional dipole magnitude

$$\delta = \sqrt{\rho_{NS}^2 + \rho_{FB}^2 + \rho_{EW}^2}. \qquad (2)$$

where the three dipole coefficients are defined as

$$\rho_{NS} = \sqrt{\frac{3}{4\pi}} a_{10} \ \rho_{FB} = \sqrt{\frac{3}{4\pi}} a_{11} \ \rho_{EW} = \sqrt{\frac{3}{4\pi}} a_{1-1} \ . \qquad (3)$$

## IV.   ANISOTROPY IN POSITRON TO ELECTRON RATIO

In Fig. 2 the results corresponding to a dipole contribution $\rho_{NS}$ in the case of positron to electron ratio are shown as function of the minimum of the energy bin. The points at every energy show no significant deviation from isotropy. Similar plots can be obtained on the amplitudes of the other dipole components. The 95% C.L. upper limits on the dipole amplitude for different energies are reported in Fig. 3. The limit obtained for the energy range from 16 to 350 GeV is $\delta < 0.020$. This limit is consistent with the one reported in [5], the only improvement due to the increased statistics after five years.

Further checks have been performed on the variation of the upper limits as function of seasons (three months time binning), looking for possible time dependence of the signal. The full data-taking period is divided into 16 seasons and the analysis is repeated on the individual samples. Even in this analysis it can be shown that no sigificant deviation from isotropy is found.

## V.   ANISOTROPY AT MAGNETOSPHERE BORDER

Since AMS is located on board of the ISS in a Low Earth Orbit (LEO), the charged CR detected by AMS before interacting with the atmosphere are exposed to the influence of the magnetosphere which deviates their trajectories denpending on their rigidities and charges. This could in principle have an effect on the measurement of the anisotropy.

In order to estimate the sensitivity to a dipole contribution due to geomagnetic effects we compared the results of the analysis at ISS altitude with the ones obtained using the asymptotic CR directions at the entrance of the magnetosphere after backtracing. We backtraced CRs from the top of AMS out to 25 Earths radii using the most recent International Geomagnetic Reference Field (IGRF) model [6] with external non-symmetric magnetic fields [7, 8], which describes the Earth magnetosphere during both quiet and active solar periods.

Since the deviation introduced by the magnetosphere with respect to the asymptotic direction depends on the CR charge, sky maps from opposite charge particles cannot be compared at magnetosphere border. The analysis described in Sec. IV
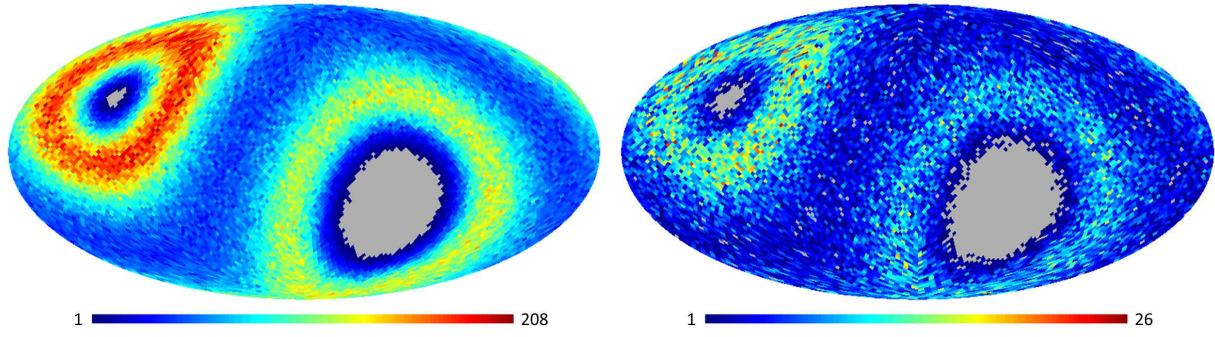
FIG. 1: Sky maps showing the arrival directions of selected electrons (left) and positrons (right) in the energy bin [16,350] GV in galactic coordinates as observed at AMS altitude. The color code reflects the number of events per bin.
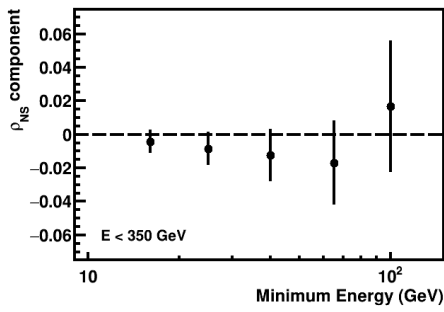


FIG. 2: Amplitudes of the $\rho_{NS}$ dipole component obtained for different energy ranges in the positron over electron case.
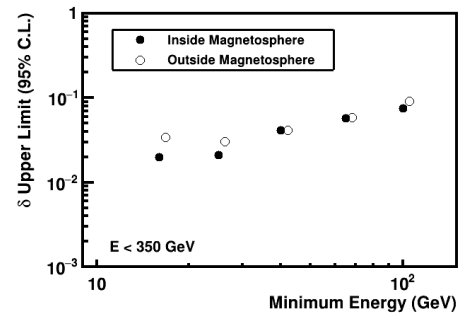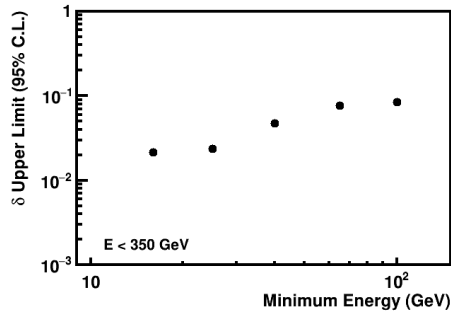


FIG. 3: Upper limits at 95% C.L. of the omnidirectional dipole intensity in the positron to electron ratio.

has thus been repeated using protons as reference for positrons, while the reference map for electrons was the proton sky map obtained after backtracing protons with negative charge.

A pure proton sample covering the same angular acceptance as the positron and electron samples is achieved by reversing the cuts on the ECAL and TRD estimators. The selected protons are classified into the energy ranges defined in Sec. IV according to their measured rigidity.



FIG. 4: Upper limits at 95% C.L. of the omnidirectional dipole intensity in the positron to proton ratio.

As reported in Fig. 4 the sensitivity to a dipole anisotropy using the positron to proton ratio is compatible with that obtained on the positron to electron analysis and the results are consistent with those presented in Sec. IV. The comparison between limits at ISS altitude and at magnetosphere border shows compatibility and no significant deviation from isotropy. Similar comments can be expressed for the results on the electron to inverted charge proton ratio reported in Fig. 5. The 95% C.L. upper limits on the dipole amplitude obtained for the energy range from 16 to 350 GeV is $\delta < 0.006$ and is completely consistent with isotropy and with the larger electron statistics with respect to positrons. The check for seasonal dependences in the results has been perfomed following the same procedure as described in Sec. IV. No seasonal variation are observed within the current statistics for both the ratios.

## VI. ANISOTROPY IN HIGH ENERGY PROTONS

The break of the proton spectra above 100GV could raise the question whether this effect can be associated to a directional dependence of the incoming energetic
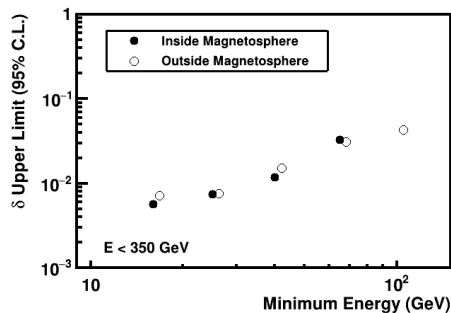
FIG. 5: Upper limits at 95% C.L. of the omnidirectional dipole intensity in the electron to inverted charge proton ratio.
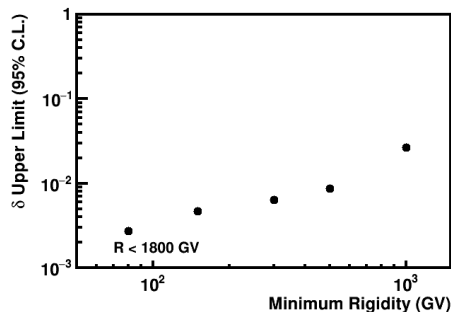


FIG. 6: Upper limits at 95% C.L. of the omnidirectional dipole intensity in the high rigidity proton to low rigidity proton ratio.

protons. In order to look for this effect the sky map of protons in the range [40,80] GV, well above geomagnetic cutoff, has been used as reference map for higher rigity protons. For this analysis protons are grouped into 5 cumulative rigidity bins from 80 to 1800 GV according to their measured rigidity. The minimum

rigidities are 80, 150, 300, 500, 1000 GV, respectively.

The 95% C.L. upper limits on the dipole amplitude for different minimium rigidities are reported in Fig. 6. The points at every rigidity show no significant deviation from isotropy. The limit obtained for the rigidity range from 80 to 1800 GV is $\delta < 0.003$. Also in this case no seasonal effects are observed.

## VII.    CONCLUSIONS

We presented the update of the results on CR anisotropy search with AMS-02 detector after five years of data taking. Within the present statistics no significant deviation from isotropy has been found in all CR species considered, both at ISS altitude and at the magnetosphere entrance. The 95% confidence level limit obtained for the energy range from 16 to 350 GeV is $\delta < 0.020$ for the positron sky map and $\delta < 0.006$ for electrons. In the case of protons the upper limit in the rigidity range from 80 to 1800 GV is $\delta < 0.003$. No indication of seasonal excess is observed on the CR anisotropy.

[1] M. Aguilar et al. (AMS Collaboration), Phys. Rev. Lett. **114**, 171103 (2015).
[2] L. Accardo et al. (AMS Collaboration), Phys. Rev. Lett. **113**, 121101 (2014).
[3] M. Aguilar et al. (AMS Collaboration), Phys. Rev. Lett. **113**, 121102 (2014).
[4] S. Ting, Nuclear Physics B - Proceedings Supplements **243244**, 12 (2013), ISSN 0920-5632, proceedings of the {IV} International Conference on Particle and Fundamental Physics in SpaceProceedings of the {IV} International Conference on Particle and Fundamental Physics in Space.
[5] M. Aguilar et al. (AMS Collaboration), Phys. Rev.

Lett. **110**, 141102 (2013).
[6] E. Thébault et al., Earth, Planets and Space **67**, 79 (2015), ISSN 1880-5981.
[7] P. Bobik, G. Boella, M. J. Boschini, M. Gervasi, D. Grandi, K. Kudela, S. Pensotti, and P. G. Rancoita, Journal of Geophysical Research: Space Physics **111**, n/a (2006), ISSN 2156-2202, a05205.
[8] N. A. Tsyganenko and M. I. Sitnov, Journal of Geophysical Research: Space Physics **110**, n/a (2005), ISSN 2156-2202, a03208.
[9] http://healpix.sourceforge.net